

1 **Tuning the Nonlinear Optical Properties of BODIPYs by**
2 **Functionalization with Dimethylaminostyryl Substituents**

3
4 Bohdan Kulyk^{a,*}, Said Taboukhat^{a,b}, Huriye Akdas-Kilig^c, Jean-Luc Fillaut^c, Miroslav Karpierz^d,
5 Bouchta Sahraoui^{a,**}

6
7 ^a*University of Angers, MOLTECH-Anjou Laboratory, UMR CNRS 6200, 2 bd Lavoisier,*
8 *49045 Angers, France*

9 ^b*Laboratory of Bio-Geosciences and Materials Engineering, ENS, University Hassan II of*
10 *Casablanca, BP 50069, Casablanca, Morocco*

11 ^c*Institut des Sciences Chimiques de Rennes, UMR CNRS 6226, University of Rennes 1,*
12 *263, avenue du General Leclerc, 35042 Rennes, France*

13 ^d*Warsaw University of Technology, Faculty of Physics, Koszykowa 75, 00-662 Warsaw,*
14 *Poland*

15
16 *Corresponding author. University of Angers, MOLTECH-Anjou Laboratory, UMR
17 CNRS 6200, 2 bd Lavoisier, 49045 Angers, France

18 **Corresponding author. University of Angers, MOLTECH-Anjou Laboratory, UMR
19 CNRS 6200, 2 bd Lavoisier, 49045 Angers, France

20 *E-mail addresses: bohdan_kulyk@yahoo.com (B. Kulyk),*

21 *bouchta.sahraoui@univ-angers.fr (B. Sahraoui)*

22

23

24 **Abstract**

25 Two difluoroboradiazaindacene (BODIPY) scaffolds with attached dimethylaminostyryl
26 substituents were synthesized. Guest-host polymeric films were produced by incorporating these
27 chromophores into polymethylmethacrylate matrices. The second and third nonlinear optical
28 properties of the resulting polymer composites were studied by means of the Maker fringe
29 technique using a laser generating at 1064 nm with a 30 ps pulse duration. The macroscopic and
30 microscopic nonlinearities were found to be comparatively high and dependent on the number of
31 dimethylaminostyryl substituents attached to BODIPY core. The development of integrated
32 optics makes such nonlinear films of particular interest, since they can be used in the creation of
33 efficient nonlinear devices.

34

35 **Keywords:** *BODIPY dye, polymer composites, second/third harmonic generation, nonlinear*
36 *susceptibility, hyperpolarizability*

37

38 **1. Introduction**

39 In recent years, difluoroboradiazaindacene (BODIPY) unit has attracted much interest
40 because of valuable spectroscopic and photophysical properties such as its high molar
41 absorptivity coefficient [1], high fluorescence quantum yield [2,3] and good stability towards
42 light and chemicals [4]. Recently many BODIPY derivatives have been synthesized and utilized
43 as fluorescent dyes [5], chemosensors [6-10], polarity sensitive probe [11], light harvesting
44 systems [12,13], and for laser applications [14] and photodynamic therapy [15,16].

45 This research work is devoted to nonlinear optical (NLO) investigations of BODIPY model
46 compounds by means of SHG and THG (second/third harmonic generation) techniques, which
47 allow the determination of second and third order NLO parameters. Until now a small set of
48 BODIPY derivatives have been investigated for nonlinear optics [17-23]. Recently, much
49 attention has been devoted to functionalized BODIPY dyes that exhibit two-photon absorption
50 (TPA) properties due to their related application in TPA imaging [24-26]. To this end, extending
51 conjugation and forming Intramolecular Charge Transfer (ICT) by means of appropriate electron
52 donor or acceptor groups are effective strategies for the synthesis of highly efficient two-photon
53 active BODIPY compounds. Thus, understanding how incorporating electron donor and/or
54 acceptor groups in the BODIPY architecture affect NLO response remains a challenge.

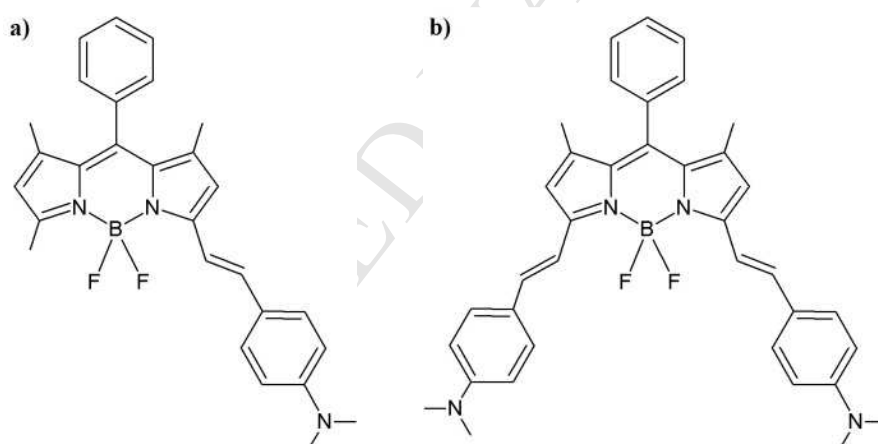
55 Our research work is focused on two BODIPY-based models which have one or two
56 dimethylaminostyryl branches, with high ICT strength from the dialkylamino-groups electron
57 donors to the electron acceptor boradipyrrin core. Interestingly, B1 and B2 models not only
58 present intrinsic “push-pull” character, but also differ by their inherent D-A (B1) and D-A-D (B2)
59 structures that potentially govern distinct second and third order optical nonlinearities. Recently,
60 we have shown that dimethylaminostyryl arms affect the nonlinear refraction and absorption
61 activity of the BODIPY structure [27]. Meanwhile, the SHG and THG study of
62 dimethylaminostyryl substituted BODIPY-based derivatives has not been done yet, so the results
63 of this investigation may extend the application range of the dye. The second and third nonlinear
64 optical properties of BODIPY-based materials, as guest-host polymeric films produced by
65 incorporating the chromophores into PMMA matrices, were studied by means of the Maker
66 fringe technique. The NLO susceptibilities and hyperpolarizabilities were extracted, which can
67 give a better understanding on the origin of NLO phenomena and the structure-property
68 relationships in BODIPY chromophores.

69 2. Experimental section

70 2.1. Materials

71 The BODIPY models have been synthesized in good yield by the established Knoevenagel
72 condensation of 3,5 dimethyl-BODIPY dyes with 4-dimethylaminobenzaldehyde, as it is
73 previously described by Rurack [28] and Akkaya [29]. The structures of the resulting
74 difluoroboradiazaindacene chromophores with dimethylaminostyryl substituents (namely B1 and
75 B2) are shown in Fig. 1. The monocondensation was controlled by adjusting the mole ratio and
76 stopping the reaction after few hours, while a larger excess of 4-dimethylaminobenzaldehyde and
77 a longer reaction time increased the yield of by-condensed product B2 (Supporting Information).

78



79
80 **Fig. 1.** Structures of the conjugated difluoroboradiazaindacene chromophores with
81 dimethylaminostyryl substituents: a) B1; b) B2.

82

83 2.2. Film fabrication

84 For the polymeric film preparation a solution of PMMA (Sigma-Aldrich, Mw=350,000
85 g/mol) dissolved in 1,1,2-trichloroethane at concentration of 50 g/L was used as a host system.

86 The concentration of the compounds was 100 μmol towards 1 g of PMMA. The glass plates were
87 washed in distilled water using ultrasonic bath, acetone, and ethanol and then dried. The solutions
88 were deposited on glass substrates using the spin-coater (SCS G3) at 1000 rpm. Obtained guest-
89 host polymer films were kept at room temperature during few days in order to eliminate any
90 remaining of solvent. The thickness of deposited films was measured with the profilometer
91 (Dektak 6M, Veeco) to be about 700 nm.

92 *2.3. Optical absorption measurements*

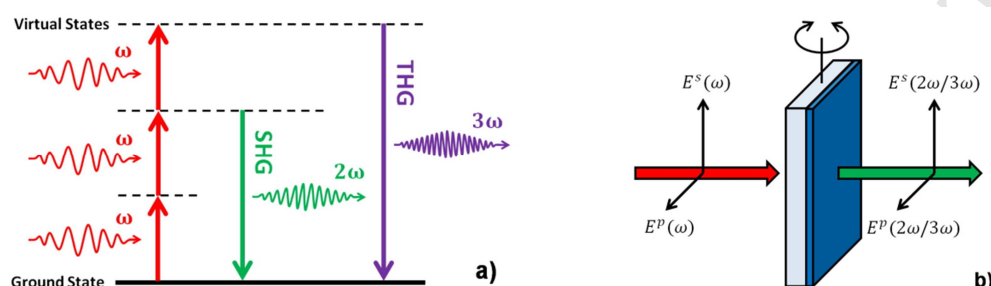
93 Absorption spectra of the B1 and B2 films were measured by means of Lambda 950
94 UV/Vis/NIR spectrophotometer (PerkinElmer) in the range 300-1200 nm. The pure PMMA film
95 on glass plate was used on the way of reference beam in spectrophotometer for the measurements
96 of absorption spectra of chromophores.

97 *2.4. SHG and THG measurements*

98 The phenomena of second and third harmonic generation (SHG and THG) may take place in
99 a material the nonlinear polarization of which, caused by intensive laser irradiation, stimulates the
100 coherent light emission at double and triple laser frequencies. The schematically energy-level
101 diagram of SHG and THG processes is shown in Fig. 2a. SHG and THG measurements were
102 performed by means of the rotational Maker fringe technique [30] in the transmission scheme for
103 the *s*- and *p*-polarized fundamental laser beams (Fig. 2b). A *y*-cut crystalline quartz plate has been
104 used as a reference material for SHG measurements and fused silica plate for THG
105 measurements. The output beam of a mode-locked Nd:YAG/YVO₄ laser (EKSPLA) generating
106 at $\lambda=1064$ nm with 30 ps pulse duration and 10 Hz repetition rate was employed as a fundamental
107 beam. The input energy of laser pulses was controlled by laser power/energy meter (LabMax

108 TOP, COHERENT) to be 90 μJ for SHG and 150 μJ for THG measurements. The detailed setups
 109 description can be found elsewhere [31].

110



111

112 **Fig. 2.** a) Energy-level diagram of SHG and THG processes and b) the illustration of input-output
 113 polarization scheme in Maker fringe experiment.

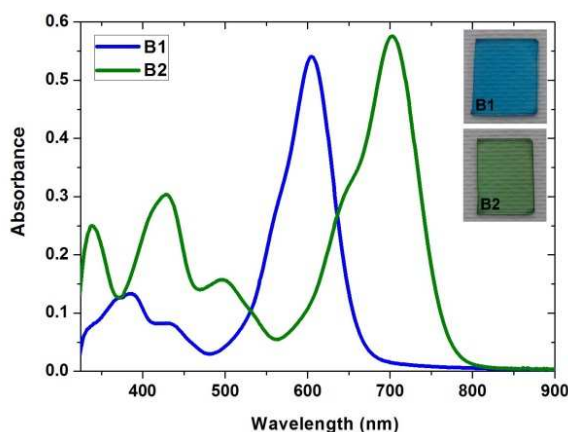
114

115 3. Results and discussion

116 3.1. Optical absorption properties

117 The absorption spectra of B1 and B2 compounds embedded in PMMA films at the
 118 concentration 100 $\mu\text{mol/g}$ are given in Fig. 3. As expected, attaching the electron donating
 119 dimethylamino groups at the 3 and 5 positions, through a conjugated bridge, leads to considerable
 120 shift of the absorption band towards the red region, by comparison with the parent BODIPY
 121 compound [2, 20]: UV-Vis (CH_2Cl_2) $\lambda_{\text{max(abs.)}} = 598 \text{ nm}$ (B1), 692 nm (B2). The UV-Vis
 122 absorption and fluorescent emission spectra of the THF solutions displayed the maximal
 123 absorbance at $\lambda_{\text{max(abs.)}} = 601 \text{ nm}$ (B1), 694 nm (B2) with a molar extinction coefficient of about
 124 90,000 $\text{M}^{-1} \text{cm}^{-1}$ and the maximal emission at $\lambda_{\text{max(em.)}} = 643 \text{ nm}$ (B1), 722 nm (B2) with the
 125 fluorescence quantum yield of 0.24 and 0.15 for B1 and B2, respectively [27]. Similarly, the
 126 spectra of both films exhibit wide absorption bands with maximum at 605 and 703 nm for B1 and

127 B2, respectively, which correspond to $S_0 \rightarrow S_1$ ($\pi-\pi^*$) transitions. The short-wavelength vibronic
 128 shoulder of these bands can be assigned to a C-H out-of-plane vibration [32]. The absorption
 129 peaks at the wavelength less than 500 nm could be attributed to a partially forbidden $S_0 \rightarrow S_2$ ($\pi-$
 130 π^*) transitions in BODIPY core [33]. As the absorption spectra indicates, introduction of second
 131 electron-donor dimethylaminostyryl group exerts almost 100 nm red-shift of absorption band
 132 without considerable change of its intensity. At the wavelengths of more than 800 nm the
 133 samples show high optical transparency.
 134

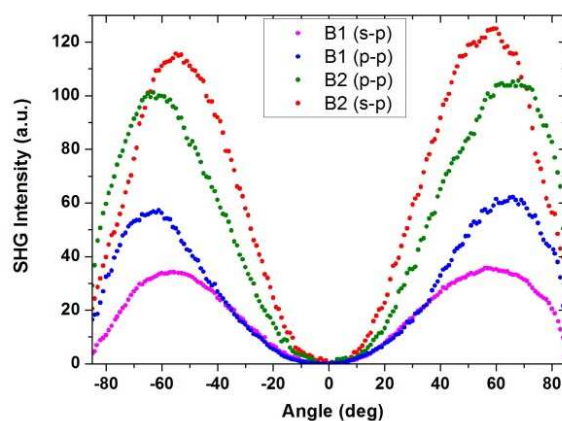


135
 136 **Fig. 3.** UV-vis absorption spectra of the B1 and B2 compounds embedded in PMMA films. In
 137 inset – the photos of the deposited films.

138 139 3.2. SHG response study

140 The rotational Maker fringe technique was implemented for the measurements of SHG in B1
 141 and B2 guest-host polymeric films for *s*- and *p*-polarized fundamental laser beam. Since the
 142 dipole moments of the chromophores are initially randomly oriented within the film, the second
 143 order nonlinear optical response of the film is negligible due to its macroscopic centrosymmetry.
 144 In order to break the centrosymmetry and induce the uniaxial orientation of NLO chromophores

145 in the polymeric films, provoking their manifestation of second order NLO behavior, the samples
 146 were corona poled just before SHG measurements. The poling temperature was 95°C, a little
 147 lower than the glass transition temperature and applied electric field was 5 kV/cm. In Fig. 4 the
 148 dependences of the second harmonic intensity generated as the function of incident angle are
 149 presented. The obtained angular dependencies are typical for induced $C_{\infty v}$ symmetry view with a
 150 maximum signal at 60°-65° and zero intensity at normal incidence of the fundamental beam. The
 151 polarization of the second harmonic signal was found to be always p -polarized regardless of the
 152 incident beam polarization due to the peculiarities of symmetry dependent second order
 153 susceptibility tensor components.
 154

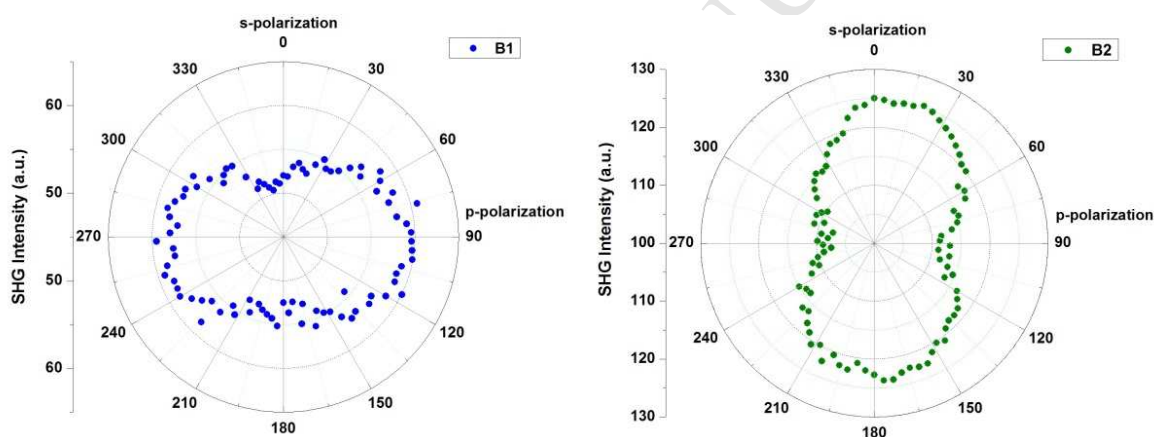


155
 156 **Fig. 4.** SHG intensity as a function of incident angle in B1 and B2 guest-host films at the s -, and
 157 p -polarized fundamental beam.

158
 159 As it can be seen for s - p or p - p polarizations, the intensity of SHG from B2 compound which
 160 has two dimethylaminostyryl units is almost two-to-three times higher than the intensity of B1
 161 with one dimethylaminostyryl unit. In contrast to B1 film, the SHG response from B2 film for s - p
 162 (input-output) polarization is higher than for p - p polarization. For B1 the higher SHG signal can

163 be obtained when the polarization of incident beam is close to parallel to its dipole moment or
 164 direction between donor (D) amine group and acceptor (A) BODIPY core, meanwhile the higher
 165 SHG signal in B2 can be obtained when the polarization of incident beam is rather perpendicular
 166 to D-A direction. In the Fig. 5 the dependences of SHG intensity on polarization of incident beam
 167 measured at 60° are presented, which confirm the contrary directions in the molecules where
 168 highest response occurs. The second order nonlinearity of BODIPY with attached
 169 dimethylaminostyryl substituents is more efficient in D-A-D architecture (B2), in which two ICT
 170 processes contribute to the NLO response, than in D-A (B1).

171



172

173 **Fig. 5.** The dependences of SHG intensity on incident beam polarization in B1 and B2 films.

174

175 Since the films have the thickness much less than their coherence length, the intensities of
 176 SHG from films were compared to that from a quartz plate and the quadratic NLO susceptibilities
 177 were calculated using following equation taking into account linear optical absorption [34]:

178

$$179 \quad \chi^{(2)} = \chi_{Quartz}^{(2)} \left(\frac{2}{\pi} \right) \left(\frac{l_{Quartz}^{coh}}{d} \right) \left(\frac{\frac{\alpha d}{2}}{1 - e^{-\frac{\alpha d}{2}}} \right) \left(\frac{I^{2\omega}}{I_{Quartz}^{2\omega}} \right)^{1/2}, \quad (1)$$

180
 181 where $\chi_{Quartz}^{(2)}$ is the quadratic susceptibility of quartz, l_{Quartz}^{coh} is the coherent length of quartz, α
 182 is the absorption coefficient at doubled laser wavelength, d is the film thickness, $I^{2\omega}$ and $I_{Quartz}^{2\omega}$
 183 are the SHG intensities from the sample and quartz under the same conditions of measurement,
 184 respectively. The obtained effective quadratic NLO susceptibilities are presented in Table 1. Here
 185 again, the effective values of $\chi^{(2)}$ for B2 compound were found to be higher than that for B1 due
 186 to the doubled amount of ICT which plays a crucial role in nonlinear behavior of a molecule. The
 187 obtained values of quadratic susceptibility are quite high and comparable with those which we
 188 have recently obtained for spin-deposited thin films of azobenzene-based push-pull compounds
 189 [35]. Meanwhile, in the microscopic approach, the first hyperpolarisabilities of B1 and B2
 190 extracted from $\chi^{(2)}$ assuming parallel orientations of dipole moment of molecules towards polar
 191 axis induced by the poling field are found to be one order of magnitude lower than for other
 192 BODIPY-based derivatives [19].

193
 194 **Table 1.** The values of $\chi_{eff}^{(2)}$, $\chi_{elec}^{(3)}$, β_{eff} and γ_{elec} obtained for B1 and B2.

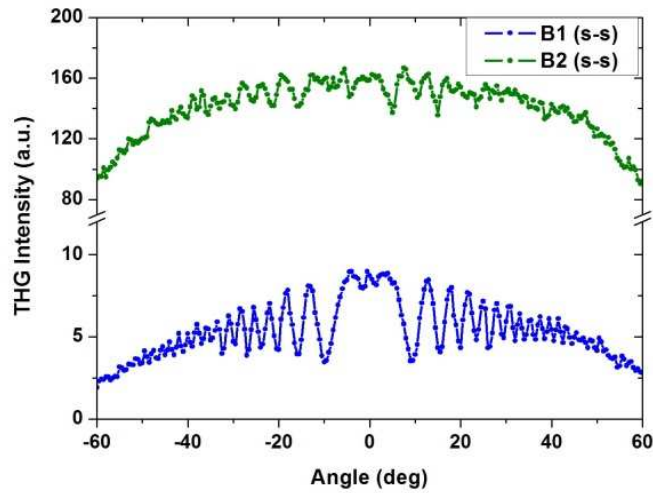
| Compound | $\chi_{eff, s-p}^{(2)}$ (pm V ⁻¹) | $\chi_{eff, p-p}^{(2)}$ (pm V ⁻¹) | β_{eff} (10 ⁻³⁸ m ⁴ V ⁻¹) | $\chi_{elec, s-s}^{(3)}$ (10 ⁻²⁰ m ² V ⁻²) | γ_{elec} (10 ⁻⁴⁷ m ⁵ V ⁻²) |
|----------|--|--|--|---|--|
| B1 | 2.75 | 3.61 | 1.86 | 0.32 | 1.16 |
| B2 | 5.86 | 5.42 | 2.79 | 1.79 | 6.37 |

195
 196 **3.3. THG response study**

197 The measurements of THG response in B1 and B2 films were performed for *s-s* incident-
 198 generated polarization scheme (Fig. 6). It can be seen that B2 film represents much higher THG

199 response compared to B1 film. As the THG originates from the film together with the glass
 200 substrate, the impact of substrate was taken into account during data processing and the cubic
 201 NLO susceptibility calculation.

202



203

204 **Fig. 6.** THG intensities from B1 and B2 films as a function of incident angle for the *s-s*
 205 polarization of the fundamental beam – generated signal.

206

207 Third order NLO susceptibility was calculated using the comparative model which takes into
 208 account linear optical absorption [36]:

209

$$210 \quad \chi^{(3)} = \chi_{Silica}^{(3)} \left(\frac{2}{\pi}\right) \left(\frac{l_{Silica}^{coh}}{d}\right) \left(\frac{\frac{\alpha d}{2}}{1 - e^{-\frac{\alpha d}{2}}}\right) \left(\frac{I^{3\omega}}{I_{Silica}^{3\omega}}\right)^{1/2}, \quad (2)$$

211

212 where $\chi_{Silica}^{(3)}$ is the cubic susceptibility of silica, l_{Silica}^{coh} is the coherent length of silica, α is the
 213 absorption coefficient at triple laser wavelength, d is the film thickness, $I^{3\omega}$ and $I_{Silica}^{3\omega}$ are the
 214 THG intensities of the samples and silica at the same conditions, respectively. The calculated

215 values of $\chi^{(3)}$ for the B1 and B2 films are given in Table 1 and they are one-to-two orders of
216 magnitude higher than for silica ($2 \cdot 10^{-20} \text{ m}^2 \text{V}^{-2}$). The compound B2 is characterized with a much
217 higher third order NLO susceptibility than B1 due to more effective electron delocalization
218 caused by charge transfers from the dimethylamino groups to the BODIPY center together with
219 its D-A-D structure, contributing to the microscopic nonlinearity.

220 The electronic contribution of second hyperpolarizability γ_{elec} for B1 and B2 molecules was
221 deducted from third order susceptibility (Table 1), as THG measurements are only dealing with
222 electronic constituent, taking into account the concentration of the molecule and the local field
223 factor [37, 38]. The comparatively higher γ_{elec} for B2 is attributed to the presence of two
224 dimethylaminostyryl substituents which imparts a greater intramolecular charge-transfer
225 character compared to B1 compound. It is worth noting that except for the intra-molecular
226 electronic contribution some role may also play vibrational contribution to hyperpolarizability of
227 the systems.

228

229 4. Conclusions

230 In summary, B1 and B2 BODIPY-based derivatives with one and two conjugated
231 dimethylaminostyryl substituents exhibit considerable second and third order NLO responses at
232 1064 nm, which can be tuned by the number of these peripheral substituents. In particular, the
233 expansion of the π -conjugated system by two electron donor groups, leading to a D-A-D
234 structure, results in significant increase of both SHG and THG responses comparing to the D-A
235 structure. Attaching strong electron-donating groups on the BODIPY core can thus promote
236 charge transfer character in these compounds and enhance their second and third order NLO
237 properties. Varying the electron donating efficiency and the respective position of donor and

238 acceptor groups in BODIPY conjugated systems will be the object of further studies with the aim
239 to establish applicable structure-property relationships.

240

241 **Acknowledgements**

242 B. K. acknowledges the Pays de la Loire region for the financial support of research work in
243 the framework of the “Molecular Systems for Nonlinear Optical Application” (MOSNOA)
244 LUMOMAT project. S. T. acknowledges the MESRSFC, IFM, and CNRST of Morocco.

245

246 **Appendix A. Supplementary data**

247 Supplementary data related to this article can be found at <http://dx.doi.org/>

248

249 **References**

- 250 [1] Guzew K, Kornowska K, Wiczek W. Synthesis and Photophysical Properties of a New
251 Amino Acid Possessing a BODIPY Moiety. *Tetrahedron Lett* 2009; 50: 2908-10.
- 252 [2] Tram K, Yan H, Jenkins HA, Vassiliev S, Bruce D. The Synthesis and Crystal Structure of
253 Unsubstituted 4,4-difluoro-4-bora-3a,4a-diaza-s-indacene (BODIPY). *Dyes Pigm* 2009; 82:
254 392-5.
- 255 [3] Arroyo IJ, Hu R, Merino G, Tang BZ, Pena-Cabrera E. The Smallest and One of the
256 Brightest. Efficient Preparation and Optical Description of the Parent Borondipyrromethene
257 System. *J Org Chem* 2009; 74: 5719-22.
- 258 [4] Haugland RP. *Handbook of fluorescent probes and research chemicals*. 9th ed. Eugene:
259 Molecular Probes Inc.; 2002.

- 260 [5] Umezawa K, Nakamura Y, Makino H, Citterio D, Suzuki K. Bright, Color-Tunable
261 Fluorescent Dyes in the Visible–Near-Infrared Region. *J Am Chem Soc* 2008; 130: 1550-51.
- 262 [6] Gabe Y, Urano Y, Kikuchi K, Kojima H, Nagano T. Highly Sensitive Fluorescence Probes
263 for Nitric Oxide Based on Boron Dipyrromethene Chromophore Rational Design of
264 Potentially Useful Bioimaging Fluorescence Probe. *J Am Chem Soc* 2004; 126: 3357-67.
- 265 [7] Qi X, Jun JE, Xu L, Kim SJ, Hong JSJ, Yoon YJ, Yoon JJ. New BODIPY Derivatives as
266 OFF–ON Fluorescent Chemosensor and Fluorescent Chemodosimeter for Cu²⁺: Cooperative
267 Selectivity Enhancement toward Cu²⁺. *J Org Chem* 2006; 71: 2881-84.
- 268 [8] Loudet A, Burgess K. BODIPY Dyes and Their Derivatives: Syntheses and Spectroscopic
269 Properties. *Chem Rev* 2007; 107: 4891-932.
- 270 [9] Lee JS, Kang NY, Kim YK, Samanta A, Feng S, Kim HK, Vendrell M, Park JH, Chang YT.
271 Synthesis of a BODIPY Library and Its Application to the Development of Live Cell
272 Glucagon Imaging Probe. *J Am Chem Soc* 2009; 131: 10077-82.
- 273 [10] Shao J, Sun H, Guo H, Ji S, Zhao J, Wu W, Yuan X, Zhang C, James TD. A highly selective
274 red-emitting FRET fluorescent molecular probe derived from BODIPY for the detection of
275 cysteine and homocysteine: an experimental and theoretical study. *Chem Sci* 2012; 3: 1049-
276 61.
- 277 [11] Duan X, Li P, Li P, Xie T, Yu F, Tang B. The Synthesis of Polarity-Sensitive Fluorescent
278 Dyes Based on the BODIPY Chromophore. *Dyes Pigm* 2011; 89: 217-22.
- 279 [12] Li F, Yang SI, Ciringh YZ, Seth J, Martin CH, Singh DL, Kim DH, Birge RR, Bocian DF,
280 Holten D, Lindsey JS. Design, Synthesis, and Photodynamics of Light-Harvesting Arrays
281 Comprised of a Porphyrin and One, Two, or Eight Boron-Dipyrrin Accessory Pigments. *J*
282 *Am Chem Soc* 1998; 120: 10001-17.

- 283 [13] Wu W, Guo H, Wu W, Ji S, Zhao J. Organic Triplet Sensitizer Library Derived from a
284 Single Chromophore (BODIPY) with Long-Lived Triplet Excited State for Triplet-Triplet
285 Annihilation Based Upconversion. *J Org Chem* 2011; 76: 7056-64.
- 286 [14] Mula S, Ray AK, Banerjee M, Chaudhuri T, Dasgupta K, Chattopadhyay S. Design and
287 Development of a New Pyrromethene Dye with Improved Photostability and Lasing
288 Efficiency: Theoretical Rationalization of Photophysical and Photochemical Properties. *J*
289 *Org Chem* 2008; 73: 2146-54.
- 290 [15] Gorman A, Killoran J, O'Shea C, Kenna T, Gallagher WM, O'Shea D. In Vitro
291 Demonstration of the Heavy-Atom Effect for Photodynamic Therapy. *J Am Chem Soc* 2004;
292 126: 10619-31.
- 293 [16] Zhao J, Wu W, Sun J, Guo S. Triplet Photosensitizers: from Molecular Design to
294 Applications. *Chem Soc Rev* 2013; 42: 5323-51.
- 295 [17] Bouit PA, Kamada K, Feneyrou P, Berginc G, Toupet L, Maury O, Andraud C. Two-Photon
296 Absorption-Related Properties of Functionalized BODIPY Dyes in the Infrared Range up to
297 Telecommunication Wavelengths. *Adv Mater* 2009; 21: 1151-4.
- 298 [18] Ulrich G, Barsella A, Boeglin A, Niu S, Ziessel R. BODIPY-Bridged Push-Pull
299 Chromophores for Nonlinear Optical Applications. *ChemPhysChem* 2014; 15: 2693-700.
- 300 [19] Shi WJ, Lo PC, Singh A, Ledoux-Rak I, Ng DKP. Synthesis and Second-Order Nonlinear
301 Optical Properties of Push-Pull BODIPY Derivatives. *Tetrahedron* 2012; 68: 8712-8.
- 302 [20] Wang Y, Zhang D, Zhou H, Ding J, Chen Q, Xiao Y, Qian S. Nonlinear Optical Properties
303 and Ultrafast Dynamics of Three Novel Boradiazaindacene Derivatives. *J Appl Phys* 2010;
304 108: 033520-8.

- 305 [21]Zhang D, Wang Y, Xiao Y, Qian S, Qian X. Long-Wavelength Boradiazaindacene
306 Derivatives with Two-Photon Absorption Activity and Strong Emission: Versatile
307 Candidates for Biological Imaging Applications. *Tetrahedron* 2009; 65: 8099-103.
- 308 [22]Potamianos D, Giannakopoulou P, Kaloudi-Chantzea A, Pistolis G, Couris, S. Third-Order
309 Nonlinear Optical Properties of Some Novel BODIPYs. *Proceedings of the 16th*
310 *International Conference on Transparent Optical Networks (ICTON)*. Graz: IEEE; 2014.
- 311 [23]Zhu M, Jiang L, Yuan M, Liu X, Ouyang C, Zheng H, Yin X, Zuo Z, Liu H, Li Y. Efficient
312 Tuning Nonlinear Optical Properties: Synthesis and Characterization of a Series of Novel
313 Poly(aryleneethynylene)s Co-Containing BODIPY. *J Polym Sci A Polym Chem* 2008; 46:
314 7401-10.
- 315 [24]Kim B, Yue X, Sui B, Zhang X, Xiao Y, Bondar MV, Sawada J, Komatsu M, Belfield KD.
316 Near-Infrared Fluorescent 4,4-Difluoro-4-bora-3a,4a-diaza-s-indacene Probes for One- and
317 Two-Photon Fluorescence Bio-imaging. *Eur J Org Chem* 2015; 2015: 5563-71.
- 318 [25]Zhang X, Xiao Y, Qi J, Qu J, Kim B, Yue X, Belfield KD. Long-Wavelength, Photostable,
319 Two-Photon Excitable BODIPY Fluorophores Readily Modifiable for Molecular Probes. *J*
320 *Org Chem* 2013; 78: 9153-60.
- 321 [26]Zhao Z, Chen B, Geng J, Chang Z, Aparicio-Ixta L, Nie H, Goh CC, Ng LG, Qin A, Ramos-
322 Ortiz G, Liu B, Tang BZ. Red Emissive Biocompatible Nanoparticles from
323 Tetraphenylethene-Decorated BODIPY Luminogens for Two-Photon Excited Fluorescence
324 Cellular Imaging and Mouse Brain Blood Vascular Visualization. *Part Part Syst Char* 2014;
325 31: 481-91.
- 326 [27]Kulyk B, Taboukhat S, Akdas-Kilig H, Fillaut J-L, Boughaleb Y, Sahraoui B. Nonlinear
327 refraction and absorption activity of dimethylaminostyryl substituted BODIPY dyes. *RSC*
328 *Adv* 2016; 6: 84854-9.

- 329 [28]Rurack K, Kollmannsberger M, Daub J. Molecular Switching in the Near Infrared (NIR)
330 with a Functionalized Boron-Dipyrromethene Dye. *Angew Chem Int Ed* 2001; 40: 385-7.
- 331 [29]Deniz E, Isbasar GC, Bozdemir ÖA, Yildirim LT, Siemiarczuk A, Akkaya EU. Bidirectional
332 Switching of Near IR Emitting Boradiazaindacene Fluorophores. *Org Lett* 2008; 10: 3401-3.
- 333 [30]Maker PD, Terhune RW, Nisenhoff M, Savage CM. Effects of Dispersion and Focusing on
334 the Production of Optical Harmonics. *Phys Rev Lett* 1962; 8: 21-2.
- 335 [31]Kulyk B, Kerasidou AP, Soumahoro L, Moussallem C, Gohier F, Frère P, Sahraoui B.
336 Optimization and Diagnostic of Nonlinear Optical Features of π -conjugated Benzodifuran-
337 Based Derivatives. *RSC Adv* 2016; 6: 14439-47.
- 338 [32]Schmitt A, Hinkeldey B, Wild M, Jung G. Synthesis of the Core Compound of the BODIPY
339 Dye Class: 4,4'-Difluoro-4-bora-(3a,4a)-diazas-indacene. *J Fluoresc* 2009; 19: 755-8.
- 340 [33]Cho DW, Fujitsuka M, Ryu JH, Lee MH, Kim HK, Majima T, Ima C. S2 Emission from
341 Chemically Modified BODIPYs. *Chem Commun* 2012; 48: 3424-6.
- 342 [34]Lee GJ, Cha SW, Jeon SJ, Jin J-I, Yoon JS. Second-Order Nonlinear Optical Properties of
343 Unpoled Bent Molecules in Powder and in Vacuum-Deposited Film. *J Korean Phys Soc*
344 2001; 39: 912-5.
- 345 [35]El Ouazzani H, Iliopoulos K, Pranaitis M, Krupka O, Smokal V, Kolendo A, Sahraoui B.
346 Second- and Third-Order Nonlinearities of Novel Push–Pull Azobenzene Polymers. *J Phys*
347 *Chem B* 2011; 115: 1944-9.
- 348 [36]Kubodera K, Kobayashi H. Determination of Third-Order Nonlinear Optical Susceptibilities
349 for Organic Materials by Third-Harmonic Generation. *Mol Cryst Liq Cryst* 1990; 182: 103-
350 13.
- 351 [37]Boyd RW. *Nonlinear Optics*. 2nd ed. Boston, Amsterdam: Academic Press; 2003.

- 352 [38] Stegeman GI, Stegeman RA. Nonlinear optics: phenomena, materials, and devices. Hoboken:
353 Wiley; 2012.

ACCEPTED MANUSCRIPT

BODIPY models with attached dimethylaminostyryl substituents were synthesized.

The nonlinear optical properties of functionalized BODIPY models were studied.

The nonlinearities are dependent on the number of dimethylaminostyryl substituents.

Electron-donating groups enhance second and third order NLO response of BODIPY.

ACCEPTED MANUSCRIPT